

A Versatile Sensor Data Processing Framework for Resource Technology

P. Kaefer^{a,b,*}, W. Oertel^b, A.D. Renno^a, P. Seidel^a, M. Meyer^a, S. Koenig^{a,b}, M. Reuter^a

^a Helmholtz-Zentrum Dresden-Rossendorf, Bautzner Landstr. 400, 01328 Dresden, Germany

^b Hochschule für Technik und Wirtschaft Dresden, Friedrich-List-Platz 1, 101069 Dresden, Germany

E-mail: p.kaefer@hzdr.de

Abstract: Novel sensors with the ability to collect qualitatively new information offer the potential to improve experimental infrastructure and methods in the field of research technology. In order to get full access to this information, the entire range from detector readout data transfer over proper data and knowledge models up to complex application functions has to be covered. The extension of existing scientific instruments comprises the integration of diverse sensor information into existing hardware, based on the expansion of pivotal event schemes and data models. Due to its flexible approach, the proposed framework has the potential to integrate additional sensor types and offers migration capabilities to high-performance computing platforms. Two different implementation setups prove the flexibility of this approach, one extending the material analyzing capabilities of a secondary ion mass spectrometry device, the other implementing a functional prototype setup for the online analysis of recyclate. Both setups can be regarded as two complementary parts of a highly topical and ground-breaking unique scientific application field. The requirements and possibilities resulting from different hardware concepts on one hand and diverse application fields on the other hand are the basis for the development of a versatile software framework. In order to support complex and efficient application functions under heterogeneous and flexible technical conditions, a software technology is proposed that offers modular processing pipeline structures with internal and external data interfaces backed by a knowledge base with respective configuration and conclusion mechanisms.

Keywords: Secondary ion mass spectrometry, recyclate analysis, resource technology, hardware framework, multi-sensor system, processing pipeline, image processing

1. Introduction	1
2. Hardware Architecture and Application Background	2
3. Software Concept	6
4. Experimental Results	10
5. Conclusion and Outlook	15

1. Introduction

Application fields like the online analysis of minerals or recyclate (OAMR) or the analysis of material composition on an isotope level using secondary ion mass spectrometry (SIMS) apply different analytical methods to understand the structure and composition of material samples. In many cases, the integration of additional sensors into the existing systems offers the potential for significant improvements of these methods. Using the OAMR example, a more comprehensive characterization of the probed material with improved analytical precision could be obtained by the use of a well-directed combination of diverse sensors, especially for highly complex, inhomogeneous samples [1], [2]. In the case of SIMS, additional components permit an increased resolution [3], [4]. While both fields use different equipment, they share the need to extract knowledge on high-dimensional sensor data. The functionality of processing, feature extraction and visualization of sensor data thus becomes a core element of the analytical method. In

4

54 order to improve the significance of material analysis, a group of researchers from HZDR
55 (Helmholtz Zentrum Dresden-Rossendorf) and HTWD (Hochschule für Technik und
56 Wirtschaft Dresden) has set up a data processing framework with a structure that can
57 process both slow control and data stream aspects for the diverse scenarios of SIMS and
58 OAMR.

59 Extending the sensor hardware and processing functionality of the aforementioned multi-
60 sensor systems raises several problems which need to be solved before a widespread
61 use in industrial applications, especially in the field of mining and recycling, is possible.
62 Both for SIMS and OAMR, the implementation of specific processing algorithms is poorly
63 prepared by industrial manufacturers. High material throughputs in OAMR result in large
64 data streams that request both fast data transfers and high processing capacity.
65 Dedicated sensor setups for visual cameras come with well-known data structures and
66 efficient algorithms; but only advanced co-registration of sensor features is able to
67 improve performance. Accurate detection crucially depends on well-designed algorithms
68 and data structures which are non-trivial in the case of a multi-sensor setup.

69 As implementation effort is a constant issue, the core idea is to arrange processing
70 modules in a flexible component-based approach. Heterogeneity of applications creates
71 the need for a flexible software extension; thus, the description of pivotal interfaces as
72 well as data representations become a crucial part of the overall design. From a software-
73 based point of view, this framework has to implement a data base for sensor
74 measurements and a knowledge base comprising reference sensor data respectively the
75 necessary background knowledge to process them. Scientific users have to build them
76 up, step by step, by expert-guided acquisition processes or system-controlled learning
77 processes.

78

79 **2. Hardware Architecture and Application Background**

80 The quality of extracted information depends to a large extent on the quality of sensor
81 hardware. Sophisticated algorithms can make best use of new sensor types and may also
82 be able to compensate the imperfections of analogue signals to the noise level, but only a
83 proper selection of sensor hardware and the extraction of high-quality primary sensor
84 information can really improve experimental results. Individual sensors require meticulous
85 preparation of their physical environment to increase the signal/noise ratio. Integrating
86 new sensors may lead to a close coupling to existing infrastructure (e.g. when extending
87 a SIMS). Another outcome may be the definition of an entirely new processing platform
88 as in the case of the OAMR [5].

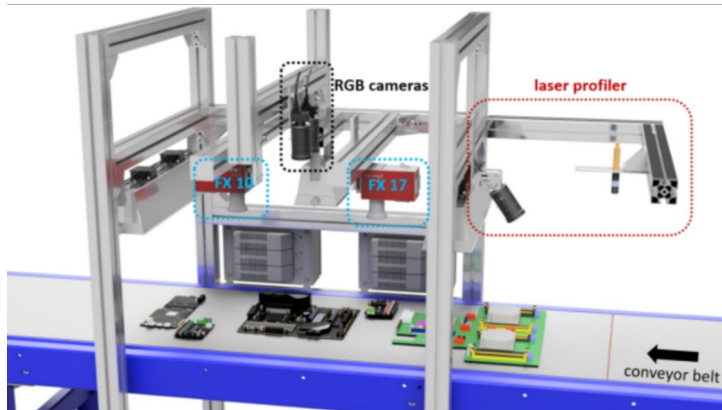
89 In both cases, sensor infrastructures have to be interfaced to different subsystems in
90 experimental hardware with regard to triggering and clocking, slow control and data
91 streaming (for complex sensors) [7], [8], [9], [10]. These subsystems can be considered
92 as being extensively independent. Clocking and trigger schemes belong to the critical
93 components in scientific instruments as they directly define the quality of analogue data
94 sampling. They depend on the physical process to an extent that no generic scheme may
95 be applied. With respect to sensors, slow control includes calibration and setting functions
96 providing all the essential preconditions for data acquisition. The aspect of data streams
97 becomes relevant for sensors with high sampling rate, often in combination with high
98 analogue resolution and channel count. In the following subsections, we will detail these
99 aspects using two experimental facilities from the OAMR and SIMS environment.

100

101 *Hardware equipment for OAMR by SenSys*

102 Recently, the SenSys system [5] has been set up as a multi-sensor system based on
103 optical spectroscopy for material flow analysis at the Helmholtz Institute Freiberg for
104 Resource Technology at HZDR (fig. 1). The mechanical hardware of SenSys consists of
105 a conveyor belt on which the sample material is placed. Conveyed samples are scanned

106 by different imaging sensors mounted above the belt and establishing different sensor
 107 sections which have to be merged. Once the material has been scanned, it runs into a
 108 collector box at the end of the conveyor belt. This setup allows for quasi-continuous
 109 operation with the belt running at speeds between 0.05 and 1 m/s.
 110



111

112 Figure 1: Schematic view of the SenSys hardware components.

113

114 The employed sensors can be divided into three groups based on their working principle.
 115 To detect the height of the individual objects, a laser profiler, consisting of a line-
 116 excitation laser (633 nm) and an RGB camera (Teledyne Dalsa Nano C4030), is used as
 117 first sensor unit. The angle between camera and laser line is set to 30°, the camera
 118 achieving a height resolution of ca. 0.4 mm. Two similar fast industry color cameras
 119 (Teledyne Dalsa Nano C4020) provide a high spatial resolution and can be combined
 120 together to create a stereoscopic image of the probed scene. Each of both cameras
 121 acquires a full frame at once. In addition, two different cameras are employed for spectral
 122 imaging of the material reflectance in a wavelength range of 400-1000 nm (Specim FX
 123 10) and 950-1700 nm (Specim FX 17) working as push-broom scanners acquiring the
 124 data line-wise, generating a total data stream of 500 MiB/s in the present setup.

125 Testing geological samples such as drill cores and rock pieces and also waste materials
 126 out of metal scrap or printed circuit boards (PCB), the performance of the data integration
 127 proved to be a powerful tool for carrying out scientific studies with the SenSys system.

128 Sensor fusion in this system is equivalent to a coherent geometric mapping of different
 129 sensors into a joined data model for further processing. Coherent stationary geometric
 130 calibration of all sensors involved is the first indispensable step. For moving objects,
 131 isometric triggering offers an efficient scheme for the mapping of both line- and 2D-
 132 cameras into a common data model. As most optical sensors provide a trigger interface,
 133 the design of a module that delivers isometric triggers was a key requirement.

134 In the case of SenSys, isometric camera triggering has been implemented using a
 135 microcontroller-based approach, delivering a belt position sampling rate of 250 kHz which
 136 leads to a special resolution of 12 micrometres at 3 m/s belt speed. Based on this signal,
 137 several trigger groups with fixed dividing frequency to the belt position increments may be
 138 defined and forwarded to the respective cameras. This proves sufficient in comparison to
 139 camera resolution and exposure time. In both cases, clocking schemes are the basis for
 140 high quality data acquisition, being configured (but not directly interfaced) via the control
 141 system.

142

143 *Material structure investigation by enhancing a conventional SIMS*

144 The analysis of the chemical composition of solids using a dynamical SIMS system [3] is
 145 essentially based on the mass spectrometric analysis of sputtered material. For this
 146 purpose, a fine-focused primary ion beam scans a precisely defined area of the sample

147 surface. The ionic fraction of the sputtered material is transferred to the mass
148 spectrometer via an elaborated ion optical system. Mass-separated ions are then
149 measured using Faraday cups or electron multipliers within a commercial CAMECA
150 7fAuto instrument; for sputtered volume determination, a white-light interferometer
151 Contour GT-K (Bruker) has been used. The SuperSIMS developed at the HZDR
152 represents a further development of this basic concept [4]. Here, only the negative mass-
153 separated secondary ions are injected into a tandem accelerator via a new unit of ion-
154 optical modules. Specific processes inside this accelerator lead to the complete
155 destruction of all molecular ions and thus to the reversal of the polarity of negative ions at
156 the terminal. As a result, molecular interferences no longer occur in the subsequent
157 analysis in the high-energy mass spectrometer, and the detection limit can be improved
158 by several orders of magnitude compared to a normal SIMS analysis. As a consequence
159 of redirecting secondary ions to detectors that are SIMS-external, the integration of
160 accelerator and detector hardware plus ion-optical sections as described in Fig. 2 prove
161 to be critical for such an enhanced instrument. Eventually this has to be enhanced by
162 extensive analytical and image generation software.

163 Consistent control can only be provided by a master control interfacing the different
164 complex components which include embedded control units, accessing the data of all
165 relevant sensors (Faraday cup, electron multiplier, image sensor) and actors (SIMS,
166 accelerator, ion optic magnets, etc.). Typically, clocking schemes provide hardware
167 synchronisation with low jitter; inside a SIMS, the detector clock thus has to be derived
168 from the primary ion beam sampling hardware on the probe. Slow control and data
169 stream interfaces are far more complex and require sophisticated techniques for
170 consistent processing - both on system and component level [8], [9], [11], [12].

171

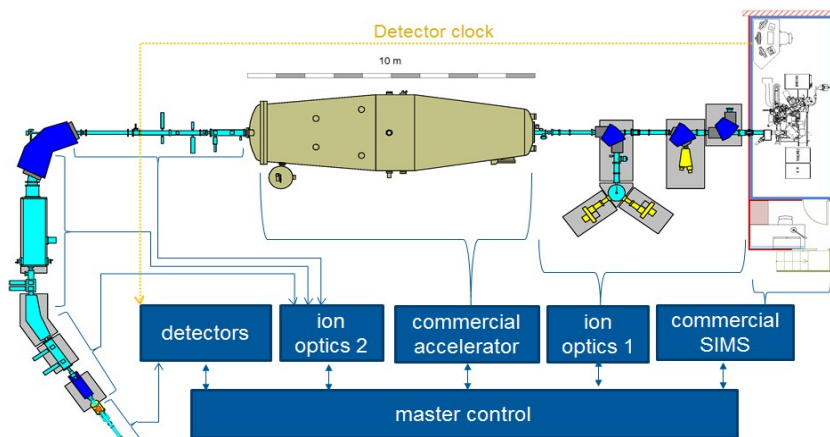
172
173
174

Figure 2: Schematic view of SuperSIMS hardware components.

175 Extending commercial SIMS equipment with new evaluation methods touches the core of
176 software architecture inside such an instrument. Under the granting of access to the
177 source code, a minimally invasive approach was the implementation of a service for the
178 distribution of raw sensor data. This allows both the preservation of the original
179 functionality and the implementation of additional interfaces with minimum processing
180 load. Among different slow control systems, the experimental physics and industrial
181 control systems (EPICS) was chosen as integration platform as it allows a representation
182 of complex subsystems (commercial SIMS, commercial accelerator and detectors) [8],
183 [9], [12]. EPICS contains a set of software tools and applications to build up a distributed
184 control system using dedicated network protocols called Channel Access (CA) and
185 pvAccess (PV) realising a client/server relationship and publish/subscribe techniques for
186 I/O-related communication. Input/output controllers (IOC) represent the device layer that

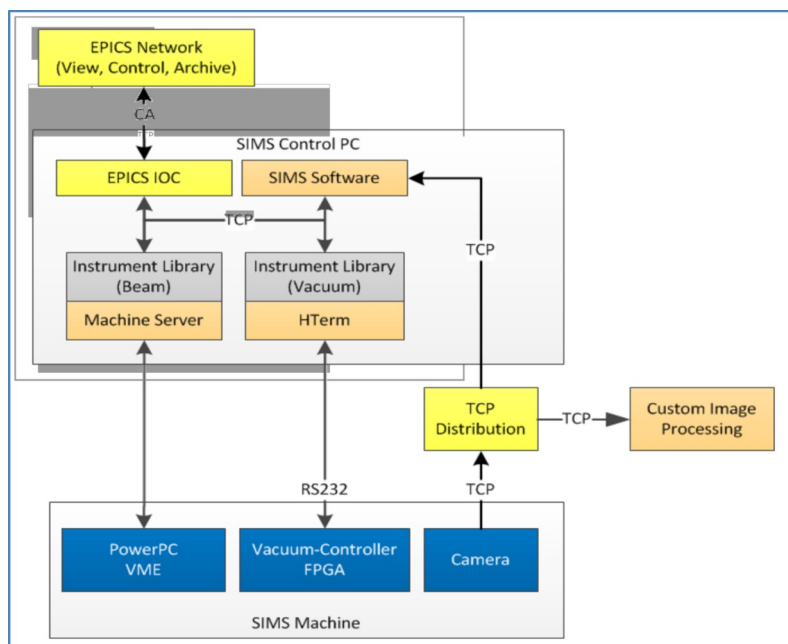
10

187 connects directly to physical I/O. EPICS is open source and used in many research
 188 facilities world-wide [8] [13]; hence, many software modules and libraries on different
 189 implementation levels are available; e.g. for graphical user interfaces, storing and
 190 accessing historical data plus IOC for particular PLC types and communication protocols
 191 like Modbus.

192 In order to integrate the existing SIMS into the EPICS control framework, its control was
 193 extended by dedicated IOCs which perform I/O-operations. It is divided between two
 194 computers - one performing realtime-tasks and another for processing and visualization.
 195 Fig. 3 shows the overview of the SIMS control with the EPICS-IOC-extension. IOC-
 196 extensions have been implemented on the visualization PC without interfering with the
 197 manufacturer's software or compromising realtime-performance. EPICS IOS's are suited
 198 to interface IO-data from the machine. Their data layout is defined by structures and
 199 enumerations that can be used to separate and convert the data into EPICS process
 200 variables and parameters. Consequently, this interface may cover the range of slow
 201 control data and prepares the setup of a master control.

202 Developing IOCs as I/O-proxies for components along the SuperSIMS beamline creates
 203 a flexible approach which consistently links data from different hardware sections into a
 204 common data base and will result in a homogeneous control system. This starts with the
 205 commercial SIMS, it will include the accelerator and extend to new detector hardware or
 206 ion-optics beamline segments. EPICS thus allows to control the SuperSIMS both
 207 manually and with the support of automation logic, e.g., it provides a framework which is
 208 able to incorporate machine safety and setup functionality.

209



210

211 Figure 3: Overview of the SIMS interfaces.

212

213 As EPICS has a focus on slow control, data streams which have to undergo elaborate
 214 processing have been handled separately. Image data streams from the SIMS detectors
 215 were interfaced applying a distinct proxy server that has been placed between the
 216 realtime-computer and the visualization PC. The proxy-server listens on the original
 217 network port, transferring the raw images from the SIMS machine to every connected
 218 peer for further processing. This preserves the functionality of the original software and
 219 pushes image data into the pipeline for analytical processing.

220 Although SuperSIMS and SenSys differ in equipment and application, the general
221 architecture of a hardware layer with inherent trigger schemes, slow control and data
222 stream interface to a processing layer is quite identical, thus motivating a generic
223 software approach for scientific data analysis.

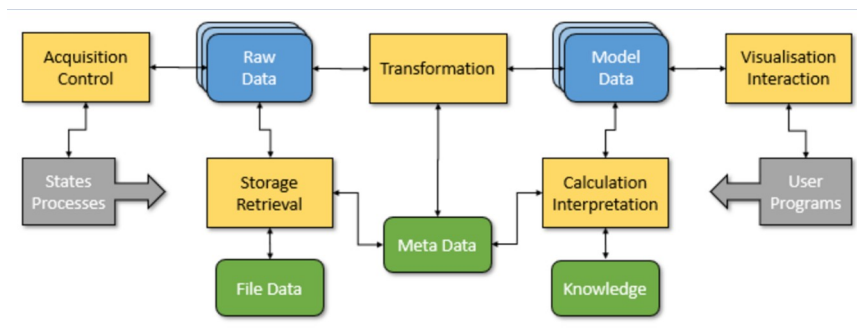
224 **3. Software Concept**

225 *Generic system architecture*

226 The basic principles of the software system necessary to support the tasks of the two
227 aimed application categories as well as to integrate the data coming from different
228 sensors or going to different actors were developed in [6]. The corresponding ASARBWG
229 project at HTWD targeted a pilot system for hardware integration and software
230 development especially for the SuperSIMS and SenSys installations. There, a vertical
231 three-layer software architecture was proposed. The central, conceptual layer defines
232 unified global data and program structures. Internal and external layers refer to different
233 efficient implementations and user interfaces, respectively. The conceptual layer with its
234 software components and relations is shown in Fig. 4. It contains horizontally three major
235 subsystems.

236 On the left, the real states and processes of the application equipment with their sensors
237 and actors are directly connected to acquisition components to deliver raw data as input
238 to the system. Vice versa, control components allow setting selected output parameters.
239 Raw data can immediately be used online or may be saved by a storage component as
240 file data for later retrieval and offline use. Depending on the context, it is fused and
241 organised in sensor- or actor-specific formats [14], [15].

242



243

244 Fig. 4: Conceptual software system structure.

245 On the right, users and other programs get information out of the system by visualisation
246 components and influence it back by interaction components. Both kinds of components
247 do not work on raw data directly, but on model data that abstract from concrete sensor
248 and actor features as well as file formats. Model data is organised along common formats
249 and unified contexts. They are also source and sink of calculation and interpretation
250 components that use domain knowledge to compute additional values or derive new
251 conclusions [16].

252 The connection between raw data and model data in both directions is provided by a set
253 of transformation components guided by metadata. Metadata is generally relevant for the
254 definition of structures and meanings of data used in the system.

255 On the internal layer, the whole system is implemented in C/C++ using OpenCV for
256 processing two- or three-dimensional image and regular data as well as VTK for
257 processing and visualizing multidimensional and structured data. For performance
258 reasons, on internal layer, OpenGL and an OpenCL-based approach [17] are involved.
259 The operating system is MS Windows for current development and Linux Ubuntu for later

260 process integration. On the external layer, a window- and a web-based user interface
261 provide access to the most important components of the system.
262 This three-layer architecture, especially the introduction of the unified conceptual layer,
263 has led to an enhanced transparency of the entire system and a substantial reduction of
264 the development and integration time for new software components which is essential for
265 an experimental system.

266

267 *Pipeline structure*

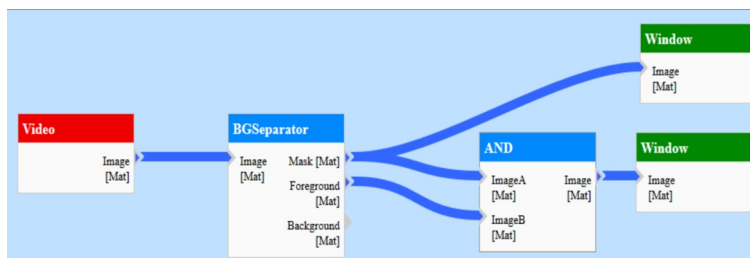
268 Because most of the data processing tasks in the developed system are considerable
269 complex, they are subdivided step by step in single operations and organised as pipelines
270 with flexible ordered or half-ordered activation structures. The result is a multiple pipeline
271 system [18], [19].

272 In such a pipeline, input data taken from a raw or model data container are computed by
273 pre-processing into prepared data as input for the content-dependent kernel
274 transformation process. At the end, the resulting transformed data is post-processed and
275 put back again as output data into a proper raw or model data container.

276 The transformation itself consists of a sequence of single operations guided by metadata
277 and knowledge to fulfil the intended task. The most important pipeline of image
278 processing consists of the steps feature extraction, region estimation, object detection
279 and scene evaluation. Another typical pipeline is data visualisation with the steps filtering,
280 mapping and rendering. Finally, problem solving pipelines apply different mathematical
281 functions, logical formula sets or rule packages in order to get conclusions by respective
282 inferences.

283 On the external layer, each pipeline has a graphical representation on the user interface.
284 Here, the operations, their parameters and their activation relations can be monitored or
285 changed interactively [20]. In this way, pipelines may also be defined by non-developers.
286 Fig. 5 shows an example pipeline on the web-based user interface where video-stream
287 image matrices are shown to be processed by a background separator; later the mask
288 and the foreground image are conjuncted and displayed in addition to the mask image.
289

289



290

291 Figure 5: Visualized example pipeline.

292

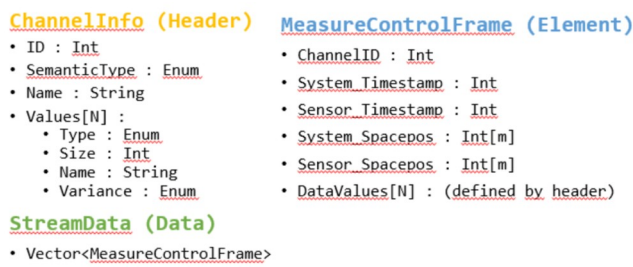
293 On the internal layer, operations can be realised using the multi-threading capability of
294 several main processors and cores or involving the massive parallelism of the graphics
295 boards. This is done manually by the programmer, but more and more automatically by
296 the image processing and visualisation libraries. The result is higher processing speed
297 and resource utilisation [21].

298 Using a generic and flexible pipeline structure allows to implement basic forms of quite
299 different - in previous systems separately realized - application components as single
300 pipelines in one system: image acquisition, process supervision, spatial count analysis,
301 profilometer viewing, knowledge-based classification, example-based learning, stereo
302 recognition, laser light section, structured light profiling and hyperspectral viewing [22],
303 [23], [24], [25], [26], [27], [28].

304

305 *Data structure*

306 Raw data is generated by the acquisition and control component and processed further
 307 on by transformation operations. In parallel, they can be stored in files and retrieved back
 308 from there. The structure of the raw data is characterised by their location in the overall
 309 system near the sensor input, respectively actor output. So, the data has to conserve the
 310 specific authentic set of original measure or control values. At the same time, it is stored
 311 in generic containers allowing certain generic operations to handle them. These two
 312 requirements are realised by organising the data in the form of an ordered vector of
 313 measure control frames in the container stream data (see fig. 6). A measure control frame
 314 is a data element with channel identifier, time stamp, space position and real data values.
 315 The role of the data values is described in the channel-information operating as data
 316 header.
 317 Using this raw data structure, image and video data produced by camera sensors in
 318 standardised formats can be managed just as vector data produced by any of the
 319 intensity or counting sensors in particular formats. Actor data is defined accordingly.
 320

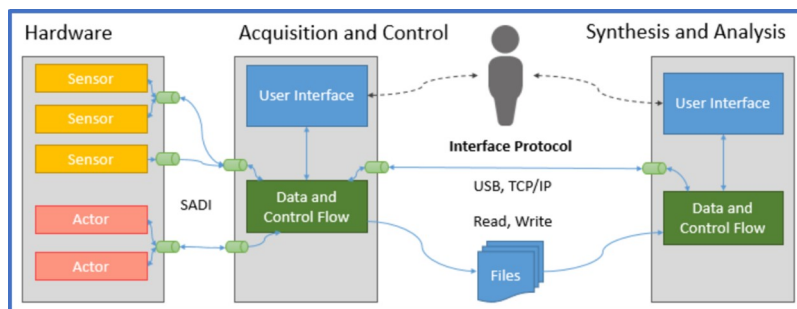


321
322 Figure 6: Sensor data format at input.

323
 324 Processing pipelines carry out complex synthesis or analysis operations. For that, they
 325 require a set of unified data structures as formatted operands and interfaces for all input,
 326 output, processing, storage, retrieval, calculation, interpretation, visualization and
 327 interaction tasks. These model data structures are formed by multi-dimensional spatial or
 328 linked graph structures organised in temporal sequences and attached by textual attribute
 329 vectors. Meta data describe the syntax and the semantics of these data.
 330 All unified data together provide the essential basis for the required flexibility,
 331 changeability and practicality of the proposed multiple pipeline system.

332
333 *Flow structure*

334 The task of the entire system can only be fulfilled efficiently if they are distributed to
 335 several cooperating components. Therefore, it is necessary that involved sensors, actors
 336 and computers are integrated with each other by a network. The essential subtask is to
 337 organise the data and the control flow among them by proper interfaces. Fig. 7 contains a
 338 schematic representation of this flow.
 339



340
341 Figure 7: Data and control flow.

343 All sensors and actors are attached by a sensor-actor-data interface (SADI). It contains
344 externally generated measure data like quantity vectors, image matrices or sensor
345 parameters as well as internally generated control data like event requests, event
346 responses or actor parameters together with precise time stamps. The conversion of
347 specific raw sensor and actor data is implemented either on hardware driver level or
348 system software level. The data transfer between processing units is handled by a client-
349 server architecture, using either the TCP/IP or the USB protocol. All the cameras are
350 integrated by Gigabit-Ethernet as in [29]. For offline work, the data-exchange is also
351 possible via read and write operations on files. This dataflow may be monitored by user
352 interfaces.

353 The performance of the entire system depends on many factors: frame sizes, frame rates
354 and number of the sensors, processing times and number of the computers, data transfer
355 times of the network, runtimes of the evaluation algorithms as well as structures and
356 number of data and knowledge elements. In our development environment at HTWD, we
357 observed cycle times for the different pipelines between 0.1 and 10.0 s, whereas the
358 lower limit is determined mainly by the network band width and camera frame sizes, the
359 upper boundary results from the combination of frame sizes and transformation
360 algorithms.

361 **4. Experimental Results**

362 While the pipelined module structure described above is able to handle both SuperSIMS
363 and SenSys applications both systems differ in data rate and processing complexity.
364 SuperSIMS provides data at much lower rate while the probed material is sputtered,
365 creating a depth profile of the scanned region with a multitude of different elements inside
366 the sputtered volume. Conversely, the multi-sensor system SenSys at HIF generates
367 much higher data rates by scanning the surface of moving samples with different
368 cameras simultaneously; each giving a defined spectral range and preferably planar
369 regionalization.

370 Both systems benefit from the presented data processing pipeline by enabling real-time
371 data streaming and full sensor control. Hardware-related issues have been addressed by
372 dedicated interface modules, creating direct access to raw images without modification of
373 proprietary firmware. Thus, after establishing the source for data streaming, we can
374 handle the streamed data according to our needs and develop flexible, customised
375 solutions for image transformation such as distortion correction, image stacking and
376 white-balancing. Moreover, the innovative design of the system software is capable to
377 incorporate diverse analysis tools. This is a great advantage compared to current
378 embedded firmware which can be modified to incorporate new sensors or functionalities
379 only with large effort.

380 Our hardware integration modules and the package of software routines overcome these
381 obstacles and will be continuously further developed to meet future tasks, e.g. the
382 incorporation of new sensors or image classification methods.

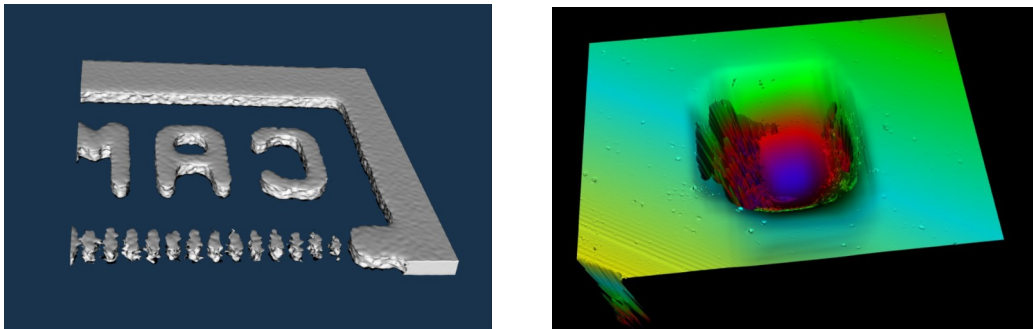
383

384 *Experimental results at SIMS material analysis*

385 Several pipeline-based programs are designed for the use in the SuperSIMS
386 environment. They are already in practical use and deliver helpful information for
387 operators and users. A dedicated software module receives raw images from a
388 commercial SIMS during the scanning process and stores these data in an open and
389 lossless file format (*.pgm). As raw-data-transformations operate on individual sensor
390 data, their processing time has been improved by multithreaded implementations for
391 multi-core-processors or GPU-mapping.

20

392 A spatial count analyser system processes the data collected by the image receiver. It
 393 interpolates counts in a volume size using a three-dimensional kernel and a marching
 394 cube algorithm for iso-surface detection. Alternatively, a volume renderer uses semi-
 395 transparent voxels and allows viewing the inside of an object. Offline 3D-volume
 396 processing is performed by reading a series of files collected by the image receiver; each
 397 representing a thin layer of material. The resulting volumes can be used to extract a 3D-
 398 surface defined by iso-detection levels of different isotopes. This allows visualizing the
 399 3D-shape of any contained substructures clearly. To look inside an object, the
 400 visualisation can be switched to be semi-transparent (fig. 8 left image).
 401



402

403

404 Figure 8: Example results for spatial count analyser (left image) and profilometer viewer (right
 405 image).
 406

407

408 Shape and volume of the real sputtered area can be inspected with the use of a Contour
 409 GT-K white-light interferometer. This unit transfers its data into a dedicated viewer system
 410 by ASC formatted files. In the viewer system, a three-dimensional surface of a sputtered
 411 material object is computed. The result can be examined from a scientific point of view
 412 with different camera points, camera perspectives, space resolutions and color mappings.
 413 A typical example for the viewer system output is the colored height profile in fig. 8 right.

414

415 Out of various analytical methods in dynamic SIMS instruments, the one which places the
 416 highest demands on the internal synchronisation inside the instrument is the
 417 measurement of the three-dimensional distribution of different elements in a precisely
 418 defined scanned area of the sample. In order to evaluate the processing of large amounts
 419 of data representing this three-dimensional distribution, e.g. in a natural mineral,
 420 measurement data were taken in the normal SIMS mode, not in the much slower Super-
 421 SIMS mode. As the data structures are identical, this approach enables the validation of
 422 the data processing pipeline. First reference tests were made on regular structures which
 423 are provided for calibration purposes. The structures are manufactured by deposition of
 424 thin tantalum layers on Si wafers. In this case, the distribution of the isotope ^{181}Ta and the
 425 molecule $^{29}\text{Si}^{30}\text{Si}$ were measured. The measurement of the element distribution in natural
 426 minerals is much more demanding. In addition to a large number of elements/isotopes to
 be measured, these are also determined at different measuring times. This corresponds

427

428 to different sputtering depths in the respective mineral.
 429 The spatial and temporal integration of sensor signals is obligatory as the process of
 430 sputtering the material sample by ion beams needs a precise spatial calibration and
 431 temporal synchronisation of all participating agents. Thus, the time of arrival of material
 432 particles must be linked to the time of sputtering on the sample because this gives the
 433 information about their former location in the material sample. At the same time, the
 434 arrival time contains information about the chemical substance because of the mass, and
 hence, acceleration and resulting velocity of the particles. Before and after the regular
 measurement, the particle flow intensity of the primary ion beam is determined as

435 reference value. The measurement of the sample itself is done with a spatial resolution of
436 up to 512x512 dots in an 80 ns time grid. The resulting particle intensities vary between 1
437 million and 1 billion per second. Fig. 9 illustrates the relationships between the sputtering
438 time path, the sample spatial grid and the global camera image.
439

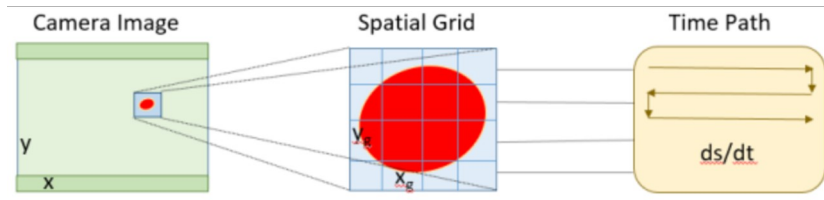
440
441
442

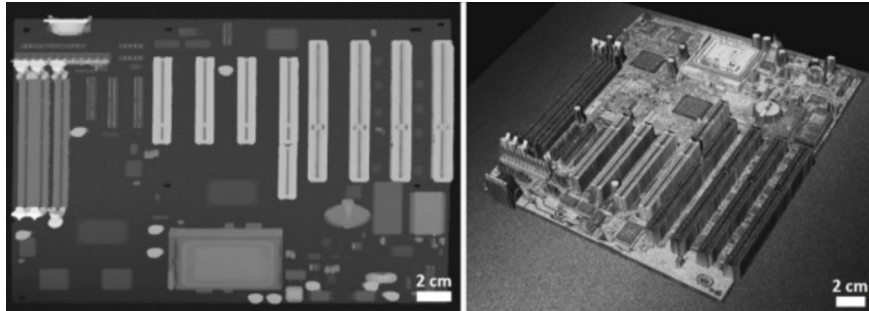
Figure 9: Image-space-time synchronisation in SuperSIMS.

443 All experimental tests prove the applicability of the developed methods and demonstrate
444 functionality and flexibility of the approach chosen here.
445 Compared to other methods of evaluating and using 3D imaging data from dynamic SIMS
446 measurements [34-36], there are several advantages.
447 The automatable detection of different matrices in the sputtered volume, combined with
448 the reconstruction of the shape and volume, allows the automatic quantification of
449 element and isotope concentrations based on the availability of matrix-matched
450 standards. This is currently only possible for measurements in exactly one matrix (e.g.
451 [34]) otherwise the element or isotope ratios are presented. The correlative automated
452 analysis of the 3D image information of the SIMS - signal and the signal of the white-light
453 interferometer allows the automated determination of the sputter rate and the analyzed
454 volumes of the individual phases. This principle makes use of additional sensors; it leads
455 to improved analytical results and can be transferred to all other methods of correlative
456 microscopy of SIMS measurements [e.g. 37].
457

458 *Experimental results for material flow analysis*

459 Using the setup of multi-sensor systems at HZDR, different material streams, especially
460 with the focus on drill cores and secondary resources (e.g. printed circuit boards and
461 metal waste) have been monitored. Besides providing classification algorithms, this work
462 resulted in two important, innovative tools for the online material stream characterization:
463 the automated object height detection by laser profiling and the streaming and pre-
464 processing of RGB color and hyperspectral reflectance images.

465 Laser light section bases on a monochrome camera together with a wavelength filter and
466 an active line laser. The software determines the deviation of a straight laser line in the
467 camera image, using triangulation to calculate the height. This approach proved to be
468 superior to stereo camera triangulation with respect to computational burden, resolution
469 and ruggedness. Applying it to a scene on a conveyor belt, a complete three-dimensional
470 surface profile (2.5D) of the moving objects in a rectangular area can be derived in real
471 time. Exemplary, in Fig. 10 two images of a reconstructed PCB are shown visualizing
472 both the preliminary height map (left) and the final 2.5D image after incorporation of the
473 greyscale reflectance and a rendering step (right). The detailed object reconstruction will
474 be further used as a base map on which the hyperspectral reflectance data projected
475 using the co-registration approach of the synchronously triggered image acquisition for
476 both hyperspectral cameras.
477



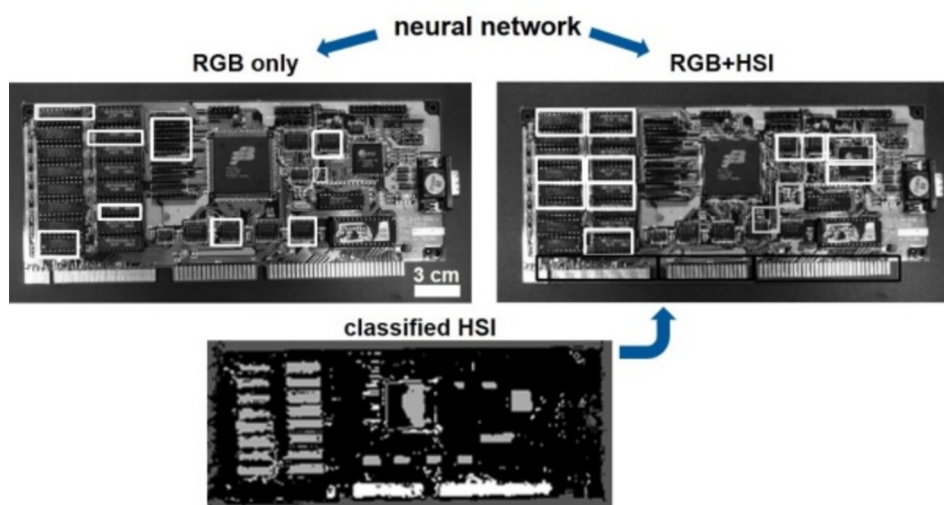
478
479 Figure 10: 2.5D-reconstructed images of the laser profiler for a PCB sample. Height map depicted
480 in grey scale with distortions in x-y directions being still uncorrected (left). Rendered 2.5D image of
481 the sample taking the greyscale values of the laser reflectance and the height information into
482 account (right).
483

484 One of the major tasks was the integration of multiple Gigabit-Ethernet cameras with
485 regard to configuration and image transfer. For example, hyperspectral (HS) cameras
486 were interfaced and their data streams have been recorded in the aforementioned pgm-
487 format with full resolution. Presently, the image streams of five cameras are processed
488 and stored which results in a data flow of 500 MB/s. The configuration part covers
489 parameters like capture regions, frame rates, trigger modes, exposure and overall
490 capture times plus gain values for image sensors and pixel bit depths. In-built raw data
491 transformations perform the change of image format, geometry and color. Raw color
492 images may be de-bayered to get RGB information or compensated for uneven spectral
493 light distribution and spotlights with a white balance algorithm.

494 Knowledge-based classification is based on camera sequence data and stored explicit
495 knowledge about elements and their relationships located on pieces of electronic circuit
496 boards. It contains image-processing steps like feature extraction, region segmentation
497 and object detection on the basis of typical object parameters like color, saturation,
498 intensity, texture, size or shape, allowing to specify their ranges or limits in dedicated
499 tables for further optimization. Typical detection rates vary between 50 and 80 %. It is
500 expected that the importance of this component will grow in future by collecting the
501 amount of real expert knowledge, also to support the other detection components.

502 Example-based classification uses a manually prepared set of reference images,
503 representing typical backgrounds, negative and positive training objects, representing
504 typical scene elements. On the base of color images, a mask extractor generates a large
505 number of assessed cropped image parts, using a multi-step cascade filter for later object
506 matching. Analysing material flows, the comparison of the high-resolution RGB image
507 with other hyperspectral reflectance sensor data has shown good results in feature
508 extraction of co-located extracted areas [5].

509 Another example of the current object detection algorithms being fed by synchronous
510 multi-camera data acquisition is the identification of PCB components with convolutional
511 neural networks (CNN) (Fig. 11). We applied the VGG-16 network architecture [24] used
512 for this task. While the network performs poorly in the detection of objects and in setting
513 the correct bounding boxes using RGB images only, we obtain an increase in accuracy
514 by taking information from the hyperspectral reflectance image into account [30]. This
515 method is inspired by the region-proposal by guided anchoring [31]. The output of the
516 supervised pixel-wise classification of the HS data is used to populate a probability map,
517 which exhibits high values where the given classes should be located. This probability
518 map is used along with the region proposal network of the CNN for the anchor
519 localization, i.e. to set the box where an object from a specific class should be detected.
520 The boxes with different grey scale color represent different object classes recognized by
521 the network in a PCB image.



523
524 Figure 11: Comparison of the object detection of PCB components by a neural network using RGB
525 images only (upper left) and RGB images combined with anchoring points from the classified
526 hyperspectral reflectance image (upper right). White boxes mark the recognition of integrated
527 circuits, grey boxes metal sheets and black boxes gold connectors. Different grey values in the
528 classified HS image represent the different detected classes (lower image).
529

530 Our approach improved the mean average precision from 0.45 to 0.61 and reduced the
531 inference time from 0.75 s to 0.32 s. Acquiring more experimental data for learning and
532 improving the network architecture should increase the accuracy of the object detection
533 and its ability to recognize a higher variety of object classes in the images.

534 The findings from the neural network dealing with different sensor data are promising
535 starting points for a further investigation of the fusion of spectral data from different
536 sources. Compared to other studies, where the fusion of RGB and hyperspectral
537 reflectance was examined [32] [33], our network is able to deal with a limited number of
538 training set and is better tailored for the application in PCB recycling. The inference times
539 are shorter due to the compression of the hyperspectral data into a low-dimensional
540 feature map. Moreover, the developed flexible software and hardware architectures
541 enable an easier and more problem-adapted integration of further sensors, which is more
542 challenging for the aforementioned other approaches. In addition, the ability of the here
543 presented pipeline for streaming large data sets provides a unique opportunity for the
544 further step of real-time multi-class object detection in material streams.
545

546 5. Conclusion and Outlook

547 The paper described a sensor data processing framework which has been applied in
548 different hardware setups in the field of resource technology, ranging from secondary-ion-
549 mass-spectrometry to optical image processing for recycle analysis. Interfacing the
550 existing hardware was inevitable groundwork to prepare the definition of new data
551 structures and processing pipelines. The use of additional sensors could thus be
552 implemented and tested on three different research and development facilities at HZDR
553 and HTWD, yielding improved analytical results compared to the original setups.

554 For a large set of equal or similar features, open source libraries could be used. The
555 present implementation allows the acquisition of raw sensor data in real time, sensor
556 fusion in a common reference system and the flexible extraction of data on different
557 processing levels for developers, experts and users.

558 This configurable processing pipeline framework serves as a base for further test and use
559 scenarios, extending the systems application-specific knowledge-base. Future work aims
560 at increasing sensitivity by integrating further sensor hardware. Extending model data and
561 knowledge structures will also improve conclusion and learning processes, resulting in
562 better material classification.
563

564 **Acknowledgments**

565 The project Asarbwg was financially supported by the Saxon State Ministry of Science
566 and Art from 2017 to 2019. We would also like to thank the involved research groups at
567 HZDR and HTW for their contributions.

568

569 **References**

570

571 [1] Gundupalli, S.; Hait, S.; Thakur, A.: A review on automated sorting of source-separated
572 municipal solid waste for recycling. *Waste management*, vol. 60, pp. 56-74, September 2016

573 [2] Robben, C.; Wotruba, H.: Sensor-based ore sorting in 2020. *AT-Autom.* 68, pp.229-230, 2020.

574 [3] Van der Heide, P.: *Secondary ion mass spectrometry*, Wiley, Hoboken, NJ, 2014

575 [4] Rugel, G. et al.: Status report of Super-SIMS for resource technology. In: *International
576 Conference on Ion Beam Analysis IBA*, Shanghai, 2017

577 [5] Lorenz, S.; Seidel, P.; Ghamisi, P.; Zimmermann, R.; Tusa, L.; Khodadazadeh, M.; Cecilia
578 Contreras, I.; Gloaguen, R.: Multi-sensor spectral imaging of geological samples: a data fusion
579 approach using spatio-spectral feature extraction. *Sensors*, 2019, 19, 2787-2810

580 [6] Oertel, W.; Kaever, P.; König, S.; Pour, R.; Renno, A. D.; Rugel, G.; Ziegenrucker, R.; Zierer,
581 R.: Software concept for automated synthesis and analysis of resource-technological image
582 data in scientific large-scale infrastructures. In: *Gesellschaft zur Förderung angewandter
583 Informatik (Hrsg.): 20. Anwendungsbezogener Workshop zur Erfassung, Modellierung,
584 Verarbeitung und Auswertung von 3D-Daten (3D-NordOst 2107)*. Gfal, Berlin, 2017; ISBN
585 978-3-942709-17-0

586 [7] Irmeler, C et al.; Run and slow control system of the Belle II silicon vertex detector; *NIMA*, 15th
587 Vienna Conference on Instrumentation, Volume: 958 Article Number: 162706 DOI:
588 10.1016/j.nima.2019.162706, Apr. 2020

589 [8] Mukai, A. H. C. et al.; Architecture of the data aggregation and streaming system for the
590 European Spallation Source neutron instrument suite; *JINST* Volume: 13 Article Number:
591 T10001 DOI: 10.1088/1748-0221/13/10/T10001; Oct. 2018

592 [9] Plackett, R.; Merlin: a fast versatile readout system for Medipix3; *JINST* Volume: 8 Article
593 Number: C01038 DOI: 10.1088/1748-0221/8/01/C01038; Jan. 2013

594 [10] Gil, A.; The slow control system of the HADES RPC wall; *NIMA* Volume: 661 Pages: S118-
595 S120 DOI: 10.1016/j.nima.2010.08.033 Supplement: 1; Jan. 2012

596 [11] Sousa, J et al.; MTCA control and data acquisition platform for Plasma Diagnostics; *JINST*
597 Volume 14 Article Number C11025, DOI: 10.1088/1748-0221/14/11/C11025; Nov. 2019

598 [12] Duckitt, W. D.; The design and implementation of a broadband digital low-level RF control
599 system for the cyclotron accelerators at iThemba LABS; *NIMA* Volume: 895 Pages: 1-9 DOI:
600 10.1016/j.nima.2018.03.064; Jul. 2018

601 [13] Feldbauer, F.; The Detector Control of the PANDA Experiment; *JINST* Volume: 9 Article
602 Number: C08025 DOI: 10.1088/1748-0221/9/08/C08025; Aug. 2014

603 [14] Jusoh, S.; Almajali, S.: A Systematic Review on Fusion Techniques and Approaches Used in
604 Applications. *IEEE Access*, 2020, Volume 8

605 [15] Karlsson, B.; Jarrhed, J.; Wide, P.: A fusion toolbox for sensor data fusion in industrial
606 recycling. *IEEE Transactions on Instrumentation and Measurement*, 2002, Volume 51

- 607 [16] Koo, S.; Kwon, H.; Yoon, C.; Seo, W.; Jung, S.: Visualization for a Multi-Sensor Data Analysis.
608 International Conference on Computer Graphics, Imaging and Visualisation (CGIV'06), 2006
- 609 [17] Rota, L. et al.: A high-throughput readout architecture based on PCI-Express Gen3 and
610 DirectGMA technology, JINST 11 P02007.; Feb. 2016
- 611 [18] Shirmohammadi, S.; Ferrero, A: Camera as the instrument: the rising trend of vision based
612 measurement. IEEE Instrumentation & Measurement Magazine, 2014, Volume 17
- 613 [19] Buckler, M.; Jayasuriya, S.; Sampson, A.: Reconfiguring the Imaging Pipeline for Computer
614 Vision. IEEE International Conference on Computer Vision (ICCV), 2017
- 615 [20] König, S.; Oertel, W.: IPSBE: Interaktives Pipeline-System für Bildverarbeitung in Echtzeit.
616 Vortrag auf der 109. Tagung der Studiengruppe Elektronische Instrumentierung (SEI). HZDR,
617 Rossendorf, 2018, ISBN: 978-3-945931-18-9 ISSN 1435-8077, pp 155-158
- 618 [21] Su, C.; Pang, H.; Liu, Y.; Ye, J.: Design of Multi-CPU Automatic Sorting System Based on
619 Machine Vision. IEEE 9th International Conference on Electronics Information and Emergency
620 Communication (ICEIEC), 2019
- 621 [22] Schnieders, A.; Budri, T.: Full wafer defect analysis with time-of-flight secondary Ion Mass
622 Spectrometry. IEEE/SEMI Advanced Semiconductor Manufacturing Conference (ASMC), 2010
- 623 [23] Ardhy, F.; Hariadi, F.: Development of SBC based machine-vision system for PCB board
624 assembly Automatic Optical Inspection. International Symposium on Electronics and Smart
625 Devices (ISESD), 2016
- 626 [24] Z. Zhao, P. Zheng, S. Xu and X. Wu, Object detection with deep learning: A review. IEEE
627 Trans. Neural Netw. Learn. Syst., vol. 30, no. 11, pp. 3212–3232, Nov. 2019
- 628 [25] Zhang, Q.; Tu, J.; Li, Z.; Liu, H.: 3D vision measurement for small devices based on consumer
629 sensors. The Journal of Engineering, 2018
- 630 [26] Yunardi, R.; Imandiri, A.: Design of The 3D Surface Scanning System for Human Wrist
631 Contour Using Laser Line Imaging. 5th International Conference on Information Technology,
632 Computer, and Electrical Engineering (ICITACEE), 2018
- 633 [27] Lilienblum, E.; Al-Hamadi, A.: A Structured Light Approach for 3-D Surface Reconstruction
634 with a Stereo Line-Scan System. IEEE Transactions on Instrumentation and Measurement,
635 2015, Volume 64
- 636 [28] Karaca, A.; Ertürk, A.; Güllü, M.; Elmas, M.; Ertürk, S.: Automatic waste sorting using
637 shortwave infrared hyperspectral imaging system. 5th Workshop on Hyperspectral Image and
638 Signal Processing: Evolution in Remote Sensing (WHISPERS), 2013
- 639 [29] He, B.; Guangsen, L.; Huawei, W.; Jia F.; Bo, G.; Hongtao, Y.: Design of multichannel data
640 acquisition system based on Ethernet. IEEE 17th International Conference on Communication
641 Technology (ICCT), 2017
- 642 [30] Sudharshan, V. et al., Object detection routine for material streams combining RGB and
643 hyperspectral reflectance data based on Guided Object Localization, IEEE Sens. J., vol. 20,
644 pp. 11490-11498, October 2020.
- 645 [31] Wang, J.; Chen, K.; Yang, S.; Loy, C.C., Lin D.: Region Proposal by Guided Anchoring, 2019
646 IEEE/CVF Conference on Computer Vision and Pattern Recognition (CVPR), pp. 2960-2969,
647 2019.
- 648 [32] Han, X.-H.; Shi, B.; Zheng, Y.Q.: SSF-CNN: Spatial and Spectral Fusion with CNN for
649 Hyperspectral Image Super-Resolution, 25th IEEE International Conference on Image
650 Processing (ICIP), October 2018.

- 651 [33] Li, M.; Hu, Y.; Zhao, N.; Qian, Q.: One-Stage Multi-Sensor Data Fusion Convolutional Neural
652 Network for 3D Object Detection, *Sensors (Basel)*, vol. 19, pp. 1434, March 2019.
- 653 [34] Li, K., Liu, J., Grovenor, C. R. M., and Moore, K. L.: NanoSIMS Imaging and Analysis in
654 *Materials Science: Annual Review of Analytical Chemistry*, v. 13, no. 1, p. 273-292, 2020,
655 <https://doi.org/10.1146/annurev-anchem-092019-032524>.
- 656 [35] Maloof, K. A., Reinders, A. N., and Tucker, K. R.: Applications of mass spectrometry imaging
657 in the environmental sciences: *Current Opinion in Environmental Science & Health*, v. 18, p.
658 54-62, 2020; <https://doi.org/https://doi.org/10.1016/j.coesh.2020.07.005>.
- 659 [36] Wirtz, T., Castro, O. D., Audinot, J.-N., and Philipp, P.: Imaging and Analytics on the Helium
660 Ion Microscope: *Annual Review of Analytical Chemistry*, v. 12, no. 1, p. 523-543, 2019;
661 <https://doi.org/10.1146/annurev-anchem-061318-115457>.
- 662 [37] Shao, C.-F., Zhao, Y., Wu, K., Jia, F.-F., Luo, Q., Liu, Z., and Wang, F.-Y.: Correlated
663 Secondary Ion Mass Spectrometry-Laser Scanning Confocal Microscopy Imaging for Single
664 Cell-Principles and Applications: *Chinese Journal of Analytical Chemistry*, v. 46, no. 7, p.
665 1005-1016, 2018; [https://doi.org/https://doi.org/10.1016/S1872-2040\(18\)61095-3](https://doi.org/https://doi.org/10.1016/S1872-2040(18)61095-3).